Mineralogical Magazine, April 2004, Vol. 68(2), pp. 231–240

Dedicated to the memory of Dr A. J. Criddle, Natural History Museum, London, who died in May 2002

Petewilliamsite, $(Ni,Co)_{30}(As_2O_7)_{15}$, a new mineral from Johanngeorgenstadt, Saxony, Germany: description and crystal structure

A. C. Roberts[1,*], P. C. Burns[2], R. A. Gault[3], A. J. Criddle[4] and M. N. Feinglos[5]

[1] Geological Survey of Canada, 601 Booth Street, Ottawa, Ontario K1A 0E8, Canada
[2] Department of Civil Engineering and Geological Sciences, 156 Fitzpatrick, University of Notre Dame, Notre Dame, Indiana 46556-0767, USA
[3] Canadian Museum of Nature, P.O. Box 3443, Station D, Ottawa, Ontario K1P 6P4, Canada
[4] Department of Mineralogy, The Natural History Museum, Cromwell Road, London SW7 5BD, UK
[5] Box 3921, Duke Medical Center, Durham, North Carolina 27710, USA

ABSTRACT

Petewilliamsite, ideally $(Ni,Co)_{30}(As_2O_7)_{15}$, monoclinic, space group $C2$, a = 33.256(5), b = 8.482(1), c = 14.191(2) Å, ß = 104.145(3)º, V = 3881.6(11) Å^3, a:b:c = 3.9209:1:1.6731, Z = 2, is a new mineral found on a single nickeline-veined quartz specimen from Johanngeorgenstadt, Saxony, Germany. The mineral possesses a pronounced subcell-supercell: a (subcell) = 1/5 a (supercell); b (subcell) = b (supercell); c (subcell) = 1/3 c (supercell), and the strongest six lines of the X-ray powder-diffraction pattern are [d in Å (I) (hkl)]: 4.235(30)(020); 3.118(100)(513, 023); 3.005(60)($\bar{1}\bar{1}$03); 2.567(50)(10$\underline{2}$0); 1.637(50)(536); 1.507(30b)(553, 1$\underline{5}$33, $\bar{2}\bar{0}$06). It occurs predominantly as scattered patches of mm-sized aggregates which are intimately associated with varicoloured xanthiosite; additional associations include bunsenite, aerugite, rooseveltite, native bismuth, paganoite and two undefined arsenates. Subhedral equant crystals with rounded faces are intimately intergrown in 1 mm-sized aggregates and individual grains do not exceed 0.5 mm in maximum diameter. The average crystal size is variable from 20 μm to 0.3 mm. The colour varies from dark violet-red to dark brownish-red and the streak is pale reddish-brown to pale purplish-brown. Crystals are translucent, brittle, vitreous, and do not fluoresce under ultraviolet light. The mineral shows neither twinning nor cleavage, has an uneven fracture, and the calculated density (for the empirical formula) is 4.904 g/cm^3. Electron-microprobe analyses gave NiO 19.45, CoO 18.39, CuO 3.40, CaO 0.17, FeO 0.04, As_2O_5 60.32, total 101.77 wt.%. The empirical formula, derived from crystal-structure analysis and electron-microprobe analyses, is $(Ni^{2+}_{14.66}Co^{2+}_{13.82}Cu^{2+}_{2.41}Ca_{0.17}Fe^{2+}_{0.03})_{\Sigma 31.09}(As^{5+}_{1.97}O_7)_{15}$, based on O = 105 atoms per formula unit (a.p.f.u.). In reflected plane-polarized light in air, petewilliamsite is dark grey with orange to spectral (multicoloured) internal reflections and no obvious bireflectance, anisotropy or pleochroism. Measured reflectance values in air are tabulated; the index of refraction calculated at 589 nm is 1.88. The mineral name honours Professor Peter ('Pete') Allan Williams of the University of Western Sydney, New South Wales, Australia, for his contributions to the study of secondary minerals.

The crystal structure of petewilliamsite has been solved by direct methods and refined on the basis of F^2 using 9212 unique reflections measured with Mo-$K\alpha$ X-radiation on a diffractometer equipped with a CCD-based detector. The final $R1$ was 7.68%, calculated for 1273 observed reflections. The structure contains 15 symmetrically distinct As^{5+} cations, each of which is tetrahedrally coordinated by four O atoms, and pairs of these AsO_4 tetrahedra share a vertex which results in As_2O_7 pyroarsenate groups that are in layers parallel to (010). The structure also has 16 distinct transition-metal M (M: Ni,Co) sites of which there are one tetrahedral, four square bipyramidal, and 11 octahedral arrangements. Adjacent pyroarsenate groups are linked through bonds to M cations. The structure of petewilliamsite is not closely related to other naturally occurring arsenates and it is the first pyroarsenate mineral.

* E-mail: aroberts@NRCan.gc.ca
DOI: 10.1180/0026461046820183

KEYWORDS: petewilliamsite, new mineral, $(Ni,Co)_{30}(As_2O_7)_{15}$, crystal structure, electron-microprobe data, reflectance data, Johanngeorgenstadt (Saxony, Germany).

Introduction

THIS unique mineral specimen, containing the new mineral described here, petewilliamsite, has an enigmatic lineage, as discussed in some detail by Roberts *et al.* (2001) which does not need be repeated here. Suffice to say that the minerals present on the specimen are unique to one locality – Johanngeorgenstadt, Saxony, Germany. This is the second new mineral described from this unusual specimen, the first being paganoite (Roberts *et al.*, 2001).

The mineral name honours Professor Peter ('Pete') Allan Williams (b. 1950), Minerals and Materials Group, School of Science, Food & Horticulture, University of Western Sydney, Penrith South DC, New South Wales, Australia, for his contributions to mineralogy, both in teaching and in research. Dr Williams, a geochemist-crystallographer, has made significant contributions to the study of secondary minerals, both in Australia and elsewhere. The mineral and name have been approved by the Commission on New Minerals and Mineral Names, IMA (2002-59). The holotype specimen still resides within the mineral collection of one of the authors (MNF) and will remain so until several undefined phases are fully characterized. Small aggregates of pure petewilliamsite in a gelatin capsule and a SEM stub have been deposited in the Systematic Reference Series of the National Mineral Collection of Canada, housed at the Geological Survey of Canada, Ottawa, Ontario, Canada, under catalogue number NMCC 68097. The polished section used for both the electron-microprobe and reflectance studies is preserved in the mineral collections at the Natural History Museum, London, UK, under catalogue number BM 2003, 6.

Occurrence and associated minerals

The bulk of the specimen, which measures $7 \times 5 \times 4$ cm and was probably mined in the mid-1800s, consists of a fine-grained quartz matrix with several veins of nickeline, NiAs, up to 4 mm thick, dispersed throughout. The nickeline veins are rimmed by native bismuth which, in turn, is rimmed by an intergrowth of very dark-green crystals of bunsenite, NiO, up to 1 mm in size. Colourful secondary minerals richly cover significant areas of the sample. These include: grass-green aerugite, $Ni_{17}As_6O_{32}$, crystals and crystal aggregates, with euhedral crystals up to 1 mm in size; varicoloured yellow to light yellow-brown to brownish purple xanthiosite, $Ni_3(AsO_4)_2$, with rare euhedral crystals up to 0.5 mm in size; colourless to white adamantine crystals of rooseveltite, $BiAsO_4$, up to 1 mm in size in several vugs; crystals and crystalline masses of orange-brown to deep golden brown paganoite, $NiBiAsO_5$, (Roberts *et al.*, 2001), intimately associated with aerugite; deep blue crusts of an undefined Ni-Co-arsenate phase, intimately associated with quartz; and an undefined Ni-Co-Cu-K-Bi-arsenate phase, which occurs as micron-sized inclusions within petewilliamsite. The new mineral is a secondary phase most likely formed from the breakdown of primary nickeline. The source of the Co and Cu is at present unknown, though perhaps the nickeline is a cobaltian variety.

Physical properties

Petewilliamsite mainly occurs in scattered patches of mm-sized aggregates, intimately associated with varicoloured xanthiosite, in an area ~1×6 cm on one edge of the specimen. Crudely crystallized petewilliamsite, in isolated patches up to 2–3 mm in size and associated with minor xanthiosite, is also found with predominant aerugite elsewhere on the specimen. Subhedral equant grains are intimately intergrown in 1 mm-sized aggregates. Crystal size is somewhat variable: in some areas, crystals average 0.3 mm in size and do not exceed 0.5 mm in maximum diameter; in other areas, crystals do not exceed 20–30 μm in size (Fig. 1). Crystal faces are rounded, but the forms are too small to determine by optical goniometry; however, they do appear complex. Twinning was not observed megascopically or in X-ray single-crystal studies. Crystals are variable in colour from dark violet-red to dark brownish-red, and the streak is pale reddish-brown to pale purplish-brown. Petewilliamsite is megascopically indistinguishable from brownish-purple xanthiosite, and we had to resort to X-ray powder-diffraction film methods in order to reliably differentiate between the two minerals.

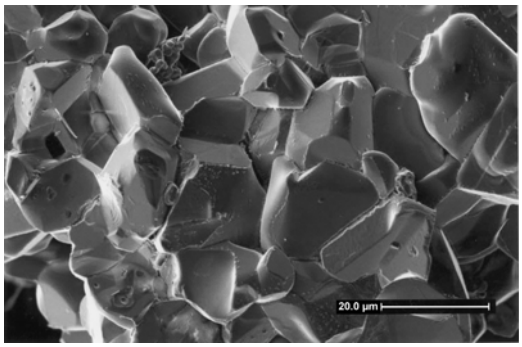

FIG. 1. SEM image of a portion of a petewilliamsite aggregate. Note the rounded nature of the crystal faces.

The lustre is vitreous and crystals are translucent. Petewilliamsite is brittle with an uneven fracture, no observable cleavage, and is non-fluorescent under both long- and short-wave ultraviolet radiation. The density could not be measured because of the small size of available crystals and dearth of material. The calculated density, on the basis of the empirical formula and unit-cell parameters derived from the crystal structure, is 4.904 g/cm^3 for Z = 2. The crystals are too small to ascertain hardness, but the mineral is soft as grains are easily crushed between two glass slides.

Reflectance studies

In plane-polarized reflected light, petewilliamsite is dark grey with no perceptible bireflectance, no anisotropy, no pleochroism and variable (from orange to spectral or multicoloured) internal reflections. Reflectance measurements in air were made relative to a Zeiss silicon carbide standard, SiC no. 472, and are presented in Table 1. The COM wavelengths are listed in bold face within the table. Reflectance measurements were also made in oil [oil index of refraction (N_D) is 1.515], but are not included in the table as they range from 0.3 to 1.0% (so that the measurement errors are of approximately the same magnitude as the measurements themselves). In the orientation of the aggregate in polished section, the mineral is sensibly isotropic and the index of refraction at 589 nm is 1.88. Vickers micro-hardness was not attempted because the material available for study was only a very small aggregate mount; VHN values obtained would not be reliable.

TABLE 1. Reflectance data for petewilliamsite.

λ (nm)	*R*	λ (nm)	*R*
400	9.84	560	9.29
420	9.85	580	9.27
440	9.71	**589**	9.27
460	9.63	600	9.26
470	9.59	620	9.29
480	9.55	640	9.33
500	9.49	**650**	9.33
520	9.39	660	9.32
540	9.33	680	9.31
546	9.32	700	9.30

Chemical composition

A petewilliamsite crystal aggregate was analysed with a JEOL 733 electron microprobe (using Tracor Northern 5500 and 5600 automation), with an operating voltage of 15 kV, a beam current of 20 nA, and a beam 10 µm in diameter. Data reduction was carried out with a PAP routine in XMAQNT (C. Davidson, CSIRO, pers. comm.). The following standards were used: synthetic $NiTa_2O_6$ (Ni-*K*α), synthetic cochromite (Co-*K*α), cuprite (Cu–*K*α), diopside (Ca-*K*α), almandine (Fe-*K*α), and olivenite (As-*L*α). A 100 s energy-dispersion scan showed no elements other than those reported; Ag, K, Sr, Mg, Mn, Bi, Pb and Zn were sought but not detected. Valency states for Ni, Co, Cu and As, as well as the number of O atoms, were determined by crystal-structure analysis prior to final normalization of the electron-microprobe data. The average of three determinations (and range) gave NiO 19.45 (19.09−19.81), CoO 18.39 (18.12−18.62), CuO 3.40 (2.93−3.98), CaO 0.17 (0.14−0.19), FeO 0.04 (0.00−0.11), As_2O_5 60.32 (59.80−60.68), total 101.77 wt.%. With O = 105, the empirical formula is $(Ni^{2+}_{14.66}Co^{2+}_{13.82}Cu^{2+}_{2.41}Ca_{0.17}Fe^{2+}_{0.03})_{\Sigma 31.09}(As^{5+}_{1.97}O_7)_{15}$. Because crystal-structure refinement could not discriminate between Ni and Co (scattering efficiencies differ by one electron), we are unable to determine what should be the ideal end-member formula at this time. An idealized formula of $(Ni_{14.1}Co_{13.5}Cu_{2.4})_{\Sigma 30}(As_2O_7)_{15}$ (with Ni:Co:Cu = 0.47:0.45:0.08) requires NiO 18.47, CoO 17.74, CuO 3.35, As_2O_5 60.45, total 100.00 wt.%.

The physical refractive energy (K_P) value is 0.1795 and is derived from the calculated index of

refraction ($\bar{n}$) of 1.88 and the calculated density of 4.904 g/cm^3. The chemical refractive energy (K_C) value is 0.1680 and is based on the empirical formula given above. The compatibility index ($1 - K_P/K_C$) is −0.068 which is rated as fair based on the classification scheme of Mandarino (1981). This somewhat mediocre compatibility is probably due to the incomplete reflectance data which, in turn, is due to the unfavourable aggregate orientation (showing isotropic as opposed to anisotropic characteristics) in polished section.

X-ray crystallography

Preliminary single-crystal precession photos of two petewilliamsite grains showed that the symmetry is monoclinic with a *C*-centred lattice and unit-cell parameters a = 6.567, b = 8.536, c = 4.721 Å, ß = 103.17º. Unfortunately, these cell parameters would not fully index the X-ray powder-diffraction pattern, particularly a number of weak reflections. The mineral possesses a very weak supercell which is only evident in the CCD-based diffraction study. The crystal-structure determination indicated that *C*2 is the correct space group; cell parameters derived from the structure determination and other pertinent information are given in Table 2. The subcell-supercell relation is as follows: a (subcell) = 1/5 a (supercell); b (subcell) = b (supercell); c (subcell) = 1/3 c (supercell). There is no obvious evidence of supercell reflections present on single-crystal precession photos. The unit-cell parameters refined from powder data, given below, are for the same orientation as those derived from the structural study.

Unit-cell parameters, a = 33.264(10), b = 8.473(2), c = 14.160(5) Å, ß = 104.15(3)º, V = 3870(2) Å^3, a:b:c = 3.9259:1:1.6712, were refined from 25 powder reflections representing d values between 4.235 and 1.413 Å for which unambiguous indexing was possible on the basis of the calculated intensities derived from the crystal structure. A fully indexed powder pattern is presented in Table 3. The majority of the d spacings, including all the strong reflections, are indexed on the subcell unit-cell parameters. The powder data are very similar to synthetic pyroarsenates $Ni_2(As_2O_7)$ (PDF 80-1177, 42-37) and $Co_2(As_2O_7)$ (PDF 80-1176).

Crystal-structure refinement

An irregular crystal of petewilliamsite (40 × 40 × 10 µm) was mounted on a Bruker PLATFORM three-circle goniometer equipped with a 1K SMART CCD (charge-coupled device) detector and a crystal-to-detector distance of 5.0 cm. A discussion of the application of CCD detectors to the analysis of mineral structures is provided by Burns (1998). A sphere of data to 58º2θ was collected using monochromatic Mo-$K\alpha$ X-radiation and frame widths of 0.3º in ω, with 20 s used to acquire each frame. The data were analysed to locate 1397 reflections for the determination of the unit-cell dimensions (Table 2), which were refined using least-squares techniques. The data were integrated using the Bruker program SAINT, and were corrected for Lorentz, polarization and background effects. A semi-empirical absorption-correction was done with the crystal modelled as

TABLE 2. Miscellaneous information pertaining to the structure determination of petewilliamsite.

a (Å)	33.256(5)	Crystal size (µm)	40 × 40 × 10
b (Å)	8.4818(14)	Radiation	Mo-$K\alpha$
c (Å)	14.191(2)	$2\theta_{max}$ (º)	56.7
β (º)	104.145(3)	Total reflections	23124
V (Å^3)	3881.6(11)	Unique reflections	9212
Space group	*C*2	Data with $\|F_o\|>4\sigma\|F_o\|$	1273
F (000)	5280	$R1$ (%)	7.68
µ (mm^{-1})	19.080	$wR2$ (%)	11.95
D_{calc} (g/cm^3)	4.873	S	1.50

h, k, l ranges: $-44 \leqslant h \leqslant 43$, $-11 \leqslant k \leqslant 11$, $-18 \leqslant l \leqslant 18$
Unit-cell contents: $2[(Ni,Co)_{30}(As_2O_7)_{15}]$

$R1 = \Sigma(|F_o| - |F_c|)/\Sigma|F_o| \times 100$
$wR2 = [\Sigma w(F_o^2\text{-}F_c^2)^2/\Sigma w(F_o^2)^2]^{½}$

TABLE 3. X-ray powder-diffraction data for petewilliamsite.

	$I_{est.}$	$d_{(meas.)}$ (Å)	$d_{(calc.)}$ (Å)	*hkl*		$I_{est.}$	$d_{(meas.)}$ (Å)	$d_{(calc.)}$ (Å)	*hkl*
	5	5.140	5.133	510	*	20	1.902	1.902	$\overline{1}026$
*	30	4.235	4.236	020		3	1.882	1.887	$\bar{8}41$
	3	3.850	3.869	$\bar{7}12$	*	10	1.769	1.771	$10\underline{4}0$
			3.861	221	*	5	1.747	1.747	$1\underline{5}13$
*	5	3.229	3.226	$\underline{1}000$	*	10	1.729	1.731	$\underline{\overline{1}}043$
	100	3.118	3.127	513		3	1.712	1.716	$\underline{\overline{1}}533$
			3.109	023	*	5	1.683	1.682	$\underline{\overline{1}}006$
*	60	3.005	3.005	$\underline{\overline{1}}003$		3	1.667	1.669	$\bar{3}51$
*	5	2.700	2.703	$\bar{9}14$		1	1.653	1.653	$\overline{2}003$
*	5	2.589	2.587	530	*	50	1.637	1.636	536
*	50	2.567	2.566	$\overline{1}020$	*	5	1.613	1.613	$\underline{2}000$
	3	2.530	2.531	822		3	1.574	1.574	$\bar{5}53$
	10	2.496	2.486	332		3	1.560	1.564	$\overline{1}026$
*	20	2.452	2.451	$\overline{1}023$				1.555	046
	10b	2.388	2.377	$\underline{1}003$	*	5	1.540	1.540	$\overline{2}023$
*	15	2.354	2.353	$\bar{5}33$		3	1.523	1.519	$\underline{1}5\overline{3}6$
	3	2.321	2.322	731				1.513	553
*	5	2.290	2.288	006		30b	1.507	1.509	$\underline{1}533$
*	20	2.258	2.260	$\bar{5}16$				1.503	$\overline{2}006$
	3	2.216	2.215	$\overline{1}\bar{3}14$				1.488	$\underline{1}714$
*	10	2.161	2.163	533		3	1.484	1.486	$\underline{\overline{2}}204$
*	5	2.121	2.118	40				1.483	$\underline{2}11\overline{5}$
*	15b	2.085	2.084	$\underline{1}510$	*	5b	1.440	1.440	$\bar{8}47$
	3	2.046	2.047	$\underline{\overline{1}}132$	*	10	1.413	1.412	060
	1	2.012	2.013	026		5	1.387	1.390	519
*	15	1.952	1.953	516				1.386	$1\underline{5}16$
*	10	1.921	1.922	043		20	1.374	1.374	$\bar{5}39$
								1.374	$\bar{5}56$

114.6 mm Debye-Scherrer powder camera ; Cu radiation, Ni filter (λ Cu-$K\alpha$ = 1.54178 Å)
– Intensities estimated visually; * = lines used for unit-cell refinement
– Not corrected for shrinkage and no internal standard; b = broad line
– Indexed on a = 33.264, b = 8.473, c = 14.160 Å, ß = 104.15º

an ellipsoid, and this lowered the R_{INT} of 960 reflections from 8.52 to 3.71%. A total of 23,124 reflections was collected, of which there were 9212 unique reflections, with 1273 classed as observed ($|F_o| \geqslant 4\sigma_F$). The Bruker SHELXTL Version 5 system of programs was used for the determination and refinement of the crystal structure. Scattering curves for neutral atoms, together with anomalous-dispersion corrections, were taken from *International Tables for X-ray Crystallography*, Vol. IV (Ibers and Hamilton, 1974).

The structure of petewilliamsite possesses a very strong monoclinic subcell with dimensions a = 6.65, b = 8.48, c = 4.73 Å, ß = 104.1º, but the correct cell is much larger and *C*-centred (Table 2). Note that the cell of synthetic $Ni_2(As_2O_7)$ is similar to the subcell found for petewilliamsite: a = 6.539, b = 8.501, c = 4.744 Å, ß = 103.2º, space group *C*2/*m* (Buckley *et al.*, 1990). The structure was solved in space group *C*2, which gave the positions of the Ni, Co and As cations. Anion positions were located in difference-Fourier maps calculated following refinement of the partial-structure model. The structure was refined on the basis of F^2 for all unique reflections. Owing to the superstructure and small crystal size, the X-ray diffraction data is weak, which imposes serious limitations when refining the structure. It was not possible to refine anisotropic-displacement parameters for the cations, or isotropic-displacement parameters for

the anions. Refinement of atom-position parameters and isotropic-displacement parameters for the cations gave an agreement index ($R1$) of 7.7%, calculated for the 1273 unique observed reflections ($|F_o| \geqslant 4\sigma_F$). Atom coordinates are listed in Table 4, and selected interatomic distances are listed in Table 5.

Description of the structure

The structure of petewilliamsite contains sixteen symmetrically distinct sites that are occupied by transition metals (designated *M*), and fifteen symmetrically distinct As sites. The coordination environments about the *M* sites are invariably

TABLE 4. Atom coordinates ($\times 10^4$) and isotropic-displacement parameters (Å^2) for petewilliamsite.

	x	*y*	*z*	U_{iso}
M(1)	0	115(11)	0	0.008(2)
M(2)	0	−6131(18)	0	0.057(4)
M(3)	2988(2)	−4884(8)	3348(5)	0.008(1)
M(4)	3957(2)	96(10)	42(4)	0.011(2)
M(5)	4029(2)	108(11)	−6690(5)	0.011(2)
M(6)	3058(2)	5075(11)	−3386(5)	0.014(2)
M(7)	4955(2)	5044(12)	−3287(5)	0.022(2)
M(8)	1995(2)	12(12)	2(6)	0.038(2)
M(9)	909(2)	5000(8)	3452(4)	0.000(1)
M(10)	3022(2)	−1227(9)	−18(5)	0.007(2)
M(11)	3994(2)	3776(8)	−3323(5)	0.015(2)
M(12)	4956(2)	−1221(10)	−6631(5)	0.008(2)
M(13)	2053(2)	−6212(10)	3289(5)	0.010(2)
M(14)	960(2)	−1187(12)	41(5)	0.021(2)
M(15)	6066(2)	3832(12)	−3408(6)	0.023(2)
M(16)	3093(2)	−1135(9)	−6787(4)	0.002(1)
As(1)	3558(1)	−3240(5)	−8027(3)	0.009(1)
As(2)	4430(1)	−3235(6)	1375(4)	0.007(1)
As(3)	3451(1)	−8251(6)	4677(4)	0.009(1)
As(4)	458(2)	−3249(7)	1331(4)	0.012(1)
As(5)	544(2)	2082(7)	1994(5)	0.020(2)
As(6)	2452(2)	−2922(8)	1348(5)	0.019(2)
As(7)	3433(2)	2072(7)	−1957(4)	0.019(2)
As(8)	2540(2)	−8237(7)	2012(4)	0.018(1)
As(9)	2427(2)	−3211(7)	4715(4)	0.010(1)
As(10)	1573(2)	−3155(7)	−1386(4)	0.019(2)
As(11)	−429(2)	6813(8)	1946(4)	0.016(2)
As(12)	3573(2)	−2948(8)	−1383(5)	0.019(2)
As(13)	4560(2)	2063(7)	−4692(5)	0.016(2)
As(14)	3546(2)	−2966(8)	5321(5)	0.024(2)
As(15)	4450(2)	−3124(8)	−5323(5)	0.023(2)
O(1)	4456(8)	−1440(40)	−5960(20)	0.020
O(2)	−791(9)	7030(40)	920(20)	0.020
O(3)	−505(8)	5310(40)	2600(20)	0.020
O(4)	4217(9)	2040(40)	−5780(20)	0.020
O(5)	3214(10)	−2920(40)	4240(20)	0.020
O(6)	4776(10)	−3050(40)	−4240(30)	0.020
O(7)	222(10)	2090(40)	900(30)	0.020
O(8)	2222(10)	−8110(40)	920(30)	0.020
O(9)	2521(9)	−4710(40)	4060(20)	0.020
O(10)	3785(10)	2000(40)	−910(30)	0.020
O(11)	2562(9)	−6470(40)	2600(20)	0.020
O(12)	3785(10)	−8140(40)	5750(30)	0.020
O(13)	4496(9)	3610(40)	−4010(20)	0.020

TABLE 4 (*contd.*).

	x	*y*	*z*	U_{iso}
O(14)	1207(10)	−2950(50)	−2400(30)	0.020
O(15)	3213(10)	−3080(40)	−9090(30)	0.020
O(16)	2792(10)	−3010(40)	5740(30)	0.020
O(17)	3492(10)	3610(50)	−2630(20)	0.020
O(18)	3529(9)	−4680(50)	5890(20)	0.020
O(19)	789(10)	−3120(50)	2410(30)	0.020
O(20)	3538(9)	−1440(50)	−700(20)	0.020
O(21)	409(9)	−1500(40)	740(20)	0.020
O(22)	3386(9)	−6510(40)	4080(20)	0.020
O(23)	3645(9)	−1530(40)	−7420(20)	0.020
O(24)	2492(9)	−1350(40)	680(20)	0.020
O(25)	556(9)	380(50)	2560(30)	0.020
O(26)	3453(9)	−4770(50)	−7370(20)	0.020
O(27)	4338(9)	−1530(40)	760(20)	0.020
O(28)	2424(9)	−4590(50)	770(30)	0.020
O(29)	558(8)	3550(40)	2640(20)	0.020
O(30)	3353(9)	580(40)	−2490(20)	0.020
O(31)	3561(8)	−9820(50)	3990(20)	0.020
O(32)	4550(8)	330(40)	−4080(20)	0.020
O(33)	4522(10)	−4720(50)	700(30)	0.020
O(34)	1508(9)	−4680(50)	−740(20)	0.020
O(35)	2361(9)	−1550(40)	4060(20)	0.020
O(36)	4785(11)	−3080(50)	2420(30)	0.020
O(37)	5000	2320(50)	−5000	0.020
O(38)	3214(11)	−3050(50)	−2420(30)	0.020
O(39)	1949(8)	−2150(30)	1314(19)	0.020
O(40)	2775(10)	−2920(50)	2450(30)	0.020
O(41)	3972(10)	−3970(30)	1560(20)	0.020
O(42)	3009(10)	−8940(40)	4970(20)	0.020
O(43)	1059(8)	2120(30)	1990(20)	0.020
O(44)	0(9)	−3950(40)	1470(20)	0.020
O(45)	548(9)	−4840(50)	670(20)	0.020
O(46)	2450(8)	−9870(50)	2720(20)	0.020
O(47)	3524(9)	−1300(50)	6030(20)	0.020
O(48)	1658(9)	−1570(40)	−850(20)	0.020
O(49)	3982(8)	−3870(40)	4700(20)	0.020
O(50)	−322(9)	8370(40)	2510(20)	0.020
O(51)	3013(9)	−8710(40)	1890(20)	0.020
O(52)	4519(8)	−4870(50)	−6030(20)	0.020
O(53)	3596(9)	−4580(40)	−760(20)	0.020

distorted, and involve one tetrahedral, four square-bipyramidal and eleven octahedral arrangements (Table 5). Each As site is coordinated by four O atoms in a tetrahedral arrangement.

The structure of petewilliamsite is closely related to those of the isostructural compounds $Ni_2(As_2O_7)$ and $Co_2(As_2O_7)$ (Buckley *et al.*, 1990). The structures of these synthetic pyroarsenates involve divalent metals in distorted octahedral coordination (Ni-O bonds: 2.05×4, 2.22×2 Å). Each octahedron shares edges with three other octahedra, resulting in a sheet of octahedra that is parallel to (001) (Fig. 2*a*). Pyroarsenate groups formed by sharing of an O atom between two arsenate tetrahedra are located between the sheets, and each of the non-bridging O atoms of the tetrahedra are shared with an octahedron in the sheet above or below (Fig. 2*b*).

The structure of petewilliamsite (Fig. 3) involves the same arrangement of pyroarsenate

TABLE 5. Selected interatomic distances (Å) and angles (º) for petewilliamsite.

M(1)–O(21)	2.03(3)	*M*(9)–O(29)	1.88(3)	As(5)–O(29)	1.55(3)
M(1)–O(21)	2.03(3)	*M*(9)–O(32)	1.96(3)	As(5)–O(7)	1.66(3)
M(1)–O(33)	2.07(3)	*M*(9)–O(12)	2.06(4)	As(5)–O(25)	1.65(4)
M(1)–O(33)	2.07(3)	*M*(9)–O(19)	2.14(4)	As(5)–O(43)	1.72(3)
M(1)–O(7)	2.13(4)	*M*(9)–O(47)	2.16(3)		
M(1)–O(7)	2.13(4)			As(6)–O(28)	1.63(4)
		M(10)–O(15)	2.04(4)	As(6)–O(40)	1.67(4)
M(2)–O(7)	1.99(4)	*M*(10)–O(8)	2.08(4)	As(6)–O(24)	1.66(4)
M(2)–O(7)	1.99(4)	*M*(10)–O(28)	2.11(4)	As(6)–O(39)	1.79(3)
M(2)–O(45)	2.14(3)	*M*(10)–O(34)	2.12(4)		
M(2)–O(45)	2.14(3)	*M*(10)–O(20)	2.17(3)	As(7)–O(30)	1.46(3)
		M(10)–O(24)	2.22(3)	As(7)–O(17)	1.66(4)
M(3)–O(22)	2.02(3)			As(7)–O(10)	1.65(3)
M(3)–O(26)	2.05(3)	*M*(11)–O(19)	2.08(4)	As(7)–O(39)	1.86(3)
M(3)–O(9)	2.06(3)	*M*(11)–O(12)	2.10(4)		
M(3)–O(11)	2.05(3)	*M*(11)–O(25)	2.11(4)	As(8)–O(8)	1.66(4)
M(3)–O(40)	2.11(4)	*M*(11)–O(18)	2.12(3)	As(8)–O(51)	1.67(3)
M(3)–O(5)	2.11(3)	*M*(11)–O(13)	2.14(3)	As(8)–O(11)	1.71(4)
		M(11)–O(17)	2.13(3)	As(8)–O(46)	1.78(4)
M(4)–O(27)	1.98(3)				
M(4)–O(20)	2.01(4)	*M*(12)–O(6)	2.05(4)	As(9)–O(9)	1.64(4)
M(4)–O(34)	2.04(3)	*M*(12)–O(36)	2.06(4)	As(9)–O(35)	1.67(4)
M(4)–O(10)	2.09(4)	*M*(12)–O(3)	2.09(3)	As(9)–O(16)	1.66(4)
M(4)–O(2)	2.11(3)	*M*(12)–O(1)	2.12(3)	As(9)–O(42)	1.73(3)
M(4)–O(45)	2.14(3)	*M*(12)–O(32)	2.15(3)		
		M(12)–O(29)	2.39(3)		
				As(10)–O(48)	1.54(3)
M(5)–O(31)	2.03(3)	*M*(13)–O(16)	2.04(4)	As(10)–O(34)	1.63(4)
M(5)–O(23)	2.00(3)	*M*(13)–O(38)	2.05(4)	As(10)–O(14)	1.66(4)
M(5)–O(1)	2.03(3)	*M*(13)–O(9)	2.10(3)	As(10)–O(51)	1.77(3)
M(5)–O(3)	2.05(3)	*M*(13)–O(11)	2.16(3)		
M(5)–O(4)	2.09(3)	*M*(13)–O(30)	2.16(3)	As(11)–O(50)	1.54(4)
M(5)–O(14)	2.12(4)	*M*(13)–O(47)	2.35(3)	As(11)–O(3)	1.64(4)
				As(11)–O(2)	1.66(3)
M(6)–O(17)	2.01(4)	*M*(14)–O(10)	2.03(4)	As(11)–O(44)	1.84(3)
M(6)–O(35)	2.03(4)	*M*(14)–O(2)	2.02(3)		
M(6)–O(38)	2.08(4)	*M*(14)–O(53)	2.09(3)	As(12)–O(20)	1.63(4)
M(6)–O(16)	2.10(4)	*M*(14)–O(33)	2.10(4)	As(12)–O(43)	1.66(3)
M(6)–O(18)	2.08(3)	*M*(14)–O(21)	2.30(3)	As(12)–O(53)	1.64(4)
M(6)–O(46)	2.13(3)			As(12)–O(38)	1.65(4)
		M(15)–O(4)	2.00(3)		
M(7)–O(50)	2.01(4)	*M*(15)–O(14)	2.05(4)	As(13)–O(37)	1.641(8)
M(7)–O(13)	2.03(3)	*M*(15)–O(26)	2.08(4)	As(13)–O(13)	1.67(4)
M(7)–O(36)	2.07(4)	*M*(15)–O(52)	2.21(3)	As(13)–O(4)	1.68(3)
M(7)–O(6)	2.10(4)	*M*(15)–O(22)	2.27(3)	As(13)–O(32)	1.71(4)
M(7)–O(52)	2.20(3)				
M(7)–O(25)	2.21(3)	*M*(16)–O(31)	2.01(3)	As(14)–O(5)	1.66(3)
		M(16)–O(40)	2.01(4)	As(14)–O(18)	1.68(4)
M(8)–O(48)	1.96(3)	*M*(16)–O(5)	2.07(3)	As(14)–O(47)	1.74(4)
M(8)–O(8)	2.07(4)	*M*(16)–O(23)	2.25(3)	As(14)–O(49)	2.02(3)
M(8)–O(24)	2.05(3)	*M*(16)–O(46)	2.34(3)		
M(8)–O(15)	2.08(4)				
M(8)–O(53)	2.70(4)				
M(8)–O(28)	2.49(4)			As(15)–O(6)	1.65(3)
				As(15)–O(49)	1.69(3)
As(1)–O(23)	1.67(4)	As(3)–O(12)	1.66(4)	As(15)–O(1)	1.69(3)
As(1)–O(15)	1.67(4)	As(3)–O(22)	1.69(4)	As(15)–O(52)	1.83(4)

TABLE 5 (*contd.*).

As(1)–O(26)	1.69(4)	As(3)–O(42)	1.73(3)
As(1)–O(41)	1.74(3)	As(3)–O(31)	1.73(4)
As(2)–O(27)	1.68(4)	As(4)–O(19)	1.66(4)
As(2)–O(36)	1.66(4)	As(4)–O(21)	1.69(4)
As(2)–O(33)	1.66(4)	As(4)–O(44)	1.69(3)
As(2)–O(41)	1.73(3)	As(4)–O(45)	1.71(4)

groups as in $Ni_2(As_2O_7)$ and $Co_2(As_2O_7)$, as well as similar sheets of MO_n polyhedra, but differs in the details of the coordination polyhedra about the divalent-metal sites. Distortion of the basic structure results in coordination polyhedra about the *M* sites ranging from distorted tetrahedral to octahedral. Substitution of a variety of transition metals at the *M* sites, as revealed by electron-microprobe analyses, presumably leads to the distortion of the structure. However, owing to the similar scattering factors for the transition metals

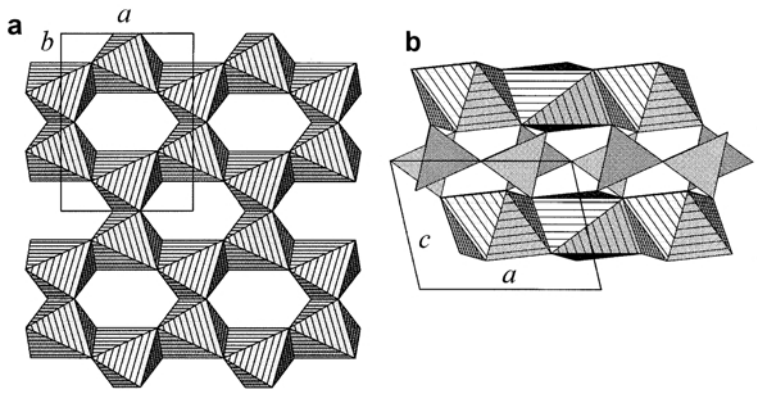

FIG. 2(*a*,*b*). Polyhedral representations of the structure of $Ni_2(As_2O_7)$ (Buckley *et al.*, 1990). NiO_6 octahedra are shaded with parallel lines, and arsenate tetrahedra are shaded solid grey.

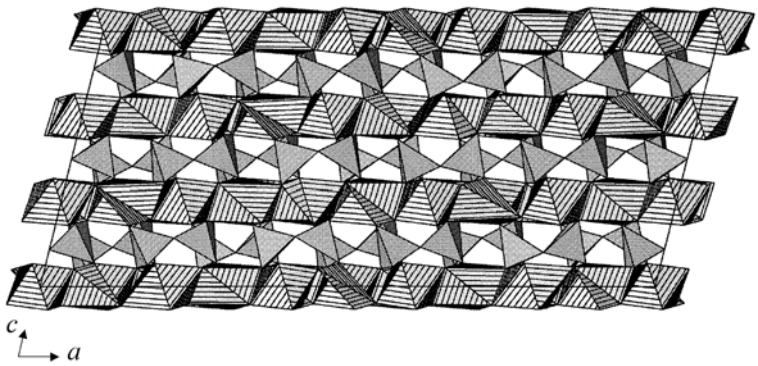

FIG. 3. Polyhedral representation of the structure of petewilliamsite. MO_n polyhedra are shaded with parallel lines, and arsenate tetrahedra are shaded solid grey.

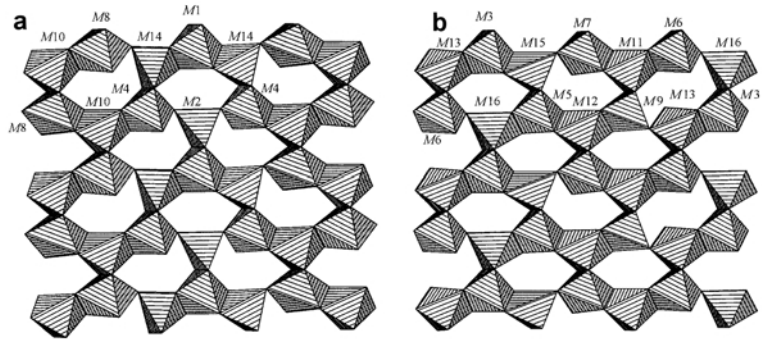

FIG. 4. Polyhedral representations of the sheets of MO_n polyhedra in the structure of petewilliamsite projected onto (110): (*a*) layer at $z \approx 0$; (*b*) layer at $z \approx 0.33$. MO_n polyhedra are shaded with parallel lines.

involved and the poor quality of the diffraction data available, it was not possible to discern ordering of cations at the *M* sites.

There are two distinct sheets of MO_n polyhedra in the structure at $z \approx 0.0$ (Fig. 4*a*) and $z \approx 0.33$ (Fig. 4*b*). The connectivities of these sheets are similar to that in $Ni_2(As_2O_7)$, except that distortions of the MO_n polyhedra in the petewilliamsite structure have resulted in polyhedral connections involving only the sharing of vertices in some cases, whereas the octahedral sheets in $Ni_2(As_2O_7)$ are linked by sharing edges.

Petewilliamsite is the only known pyroarsenate mineral. It is not closely related to any other known mineral, although >20 synthetic pyroarsenates are known.

Acknowledgements

The senior author wishes to thank Ms Pat Hunt (GSC) for the SEM photomicrograph reproduced in Fig. 1, Ms Kathryn Mooney (GSC) for typing the manuscript, and F.C. Hawthorne (University of Manitoba) for reviewing the manuscript.

References

Buckley, A.M., Bramwell, S.T. and Day, P. (1990) Structural Properties of Transition Metal Pyroarsenates MAs_2O_7 (*M*=Co,Mn,Ni). *Journal of Solid State Chemistry*, **86**, 1–15.

Burns, P.C. (1998) CCD area detectors of X-rays applied to the analysis of mineral structures. *The Canadian Mineralogist*, **36**, 847–853.

Ibers, J.A. and Hamilton, W.D. (editors) (1974) *International Tables for X-ray Crystallography*, **IV**. The Kynoch Press, Birmingham, UK.

Mandarino, J.A. (1981) The Gladstone-Dale relationship: Part IV. The compatibility concept and its application. *The Canadian Mineralogist*, **19**, 441–450.

Roberts, A.C., Burns, P.C., Gault, R.A., Criddle, A.J. and Feinglos, M.N. (2001) Paganoite, $NiBi^{3+}As^{5+}O_5$, a new mineral from Johanngeorgenstadt, Saxony, Germany: description and crystal structure. *European Journal of Mineralogy*, **13**, 167–175.

[*Manuscript received 12 August 2003: revised 13 September 2003*]